

Article

Cu Metallization of Al₂O₃ Ceramic by Coating Deposition from Cooled- and Hot-Target Magnetrons

Andrey V. Kaziev ^{1,*} , Dobrynya V. Kolodko ^{1,2} , Vladislav Yu. Lisenkov ¹, Alexander V. Tumarkin ¹, Maksim M. Kharkov ¹ , Nikolay N. Samotaev ³ and Konstantin Yu. Oblov ³

¹ Institute for Laser and Plasma Technologies, National Research Nuclear University MEPhI, 115409 Moscow, Russia

² Kotelnikov Institute of Radio Engineering and Electronics RAS, Fryazino Branch, 141190 Fryazino, Russia

³ Institute of Nanoengineering in Electronics, Spintronics and Photonics, National Research Nuclear University MEPhI, 115409 Moscow, Russia

* Correspondence: kaziev@plasma.mephi.ru

Abstract: We examined the feasibility of alumina substrate metallization by magnetron deposition of copper coatings with thickness of several tens μm for its prospective applications in production of ceramic PCBs and packaging. The films were prepared in magnetron sputtering systems with cooled and thermally insulated (hot) targets. Substrates with different geometries were used, including those with through-holes. Thickness, adhesive properties, and electrical resistivity of produced coatings were analyzed. If the film thickness exceeded ~20 μm, we observed its systematic delamination, unless the dedicated Cu_xO_y sub-layer of was introduced between the substrate and the main Cu film. Intermediate copper oxide films were investigated separately by SEM, EDS, and XRD methods, and deposition conditions for predominant growth of favorable tenorite CuO were determined. Prepared composite two-layer CuO + Cu coatings with total thickness of ~100 μm demonstrated good adhesion to alumina substrates in scratch-testing and performed much better than Cu-only films both in soldering and thermal cycling tests. We discuss an approach for constructing a reliable metallizing coating by plasma-assisted PVD methods that could be beneficial for complex-shaped ceramic PCBs and packaging.

Keywords: magnetron; sputtering; evaporation; copper; alumina; ceramic PCB; ceramic packaging



Citation: Kaziev, A.V.; Kolodko, D.V.; Lisenkov, V.Y.; Tumarkin, A.V.; Kharkov, M.M.; Samotaev, N.N.; Oblov, K.Y. Cu Metallization of Al₂O₃ Ceramic by Coating Deposition from Cooled- and Hot-Target Magnetrons. *Coatings* **2023**, *13*, 238. <https://doi.org/10.3390/coatings13020238>

Academic Editor: Csaba Balázs

Received: 31 October 2022

Revised: 16 January 2023

Accepted: 17 January 2023

Published: 19 January 2023



Copyright: © 2023 by the authors. Licensee MDPI, Basel, Switzerland. This article is an open access article distributed under the terms and conditions of the Creative Commons Attribution (CC BY) license (<https://creativecommons.org/licenses/by/4.0/>).

1. Introduction

Ceramic printed circuit boards (PCBs) and ceramic semiconductor packages are crucial components of many modern electronic devices. They are widely used in fabrication of sensors [1–3] and are almost a non-alternative option for production of high-power IGBT modules, MOSFET devices, state-of-the-art radiofrequency, and microwave integrated circuits [4–14].

The main requirements for the boards are their ability to transmit electrical signal without interruptions between the electronic device components and long service life. The latter can be guaranteed if the boards are manufactured in accordance with the conditions relevant to those they would be subjected to during real operation.

For high-power and/or microwave electronics, the issue of module heating is especially topical. Growing demands for technological characteristics of devices, boosting their productivity, while minimizing the size of a module, which results in intense Ohmic heating of PCBs and/or packaging during operation. Heating to a critical temperature or its high-magnitude periodic changes (thermal cycling) inevitably result in failure of the electronic module [4]. This happens mainly due to the difference in the coefficient of linear thermal expansion (CLTE) of the dielectric and conductor materials used in the PCB manufacturing. Thus, the service life of PCBs and packaging largely depends on the quality of connection and adhesion between the conductor and the dielectric. Therefore, the quality

of bonding can be improved by selecting proper pair of conductor and dielectric materials, and by choosing the suitable method of their joining.

The use of materials with good thermal conductivity is required for efficient heat removal in order to prevent overheating. Hence, the conductors are usually made from metals, such as copper, silver, gold, and aluminum, due to their high electric and thermal conductivity. The dielectric material can be selected from a list of various ceramics (aluminum oxide, aluminum nitride, silicon nitride, silicon carbide, and others) that are characterized by good electrical insulation and have more or less similar thermal conductivity coefficient as the metal part.

One of the most common dielectric–conductor combinations for PCBs in high-power electronics is alumina ceramics with copper, since these materials have small difference in CLTE ($8.0 \times 10^{-6} \text{ K}^{-1}$ for Al_2O_3 vs. $16.8 \times 10^{-6} \text{ K}^{-1}$ for Cu). Additionally, the use of aluminum oxide is less demanding than that of aluminum nitride, while copper is much cheaper than silver or gold. For these reasons, we consider only this pair of materials. Nevertheless, the difference in thermal conductivity between alumina and copper is considerably high ($25\text{--}30 \text{ W/m} \times \text{K}$ for Al_2O_3 vs. $384\text{--}410 \text{ W/m} \times \text{K}$ for Cu) that implies inferior thermal dissipation and accumulation of unwanted heat in the interface region. For high-power electronic devices, the copper layer must be thick enough ($>100 \mu\text{m}$) to have acceptable electrical conductivity. However, the thicker the layer, the worse the adhesion due to higher mechanical stresses [15].

The main methods that can be used to form metallizing copper layers on alumina are active metal brazing (AMB), thermal spraying (TS) and cold gas-dynamic spraying (CGS), direct bonded copper (DBC), thick film technology (low temperature (LTCC), high temperature (HTCC) co-fired ceramic), and thin film technology (vacuum evaporation, sputter deposition and their variations).

In AMB, the problem of CLTE mismatch is solved by preparation of intermediate layers of active metals or their mixtures between thick copper layer and the substrate. They are used to reduce stresses that evolve in the metal-ceramic joint during temperature fluctuations [5]. Apart from introducing an additional layer with individual thermal and electrical properties, the disadvantages of AMB technology are the difficulties in selecting operating modes for main coating deposition/electroplating and the high cost of equipment.

In CGS, an intermediate layer is sprayed on the ceramic substrate prior to metallization, as well. The processing temperature can be low since no thermal energy is involved, and the whole plating process is executed under the influence of kinetic energy of particles [16,17]. The advantages of the CGS technology are low cost, manufacturability, and high metallization rate. The main drawback is the presence of an additional layer between the coating and the substrate, which decreases thermal conductivity, hence main copper coating shows poor adhesive properties in thermal cycling. Therefore, CGS is not a good choice for a high-power component PCB production.

DBC is the most widely used technology for producing thick copper films ($100\text{--}700 \mu\text{m}$) on ceramic substrates. The mechanism of establishing strong copper–alumina connection in DBC is eutectic bonding and mutual diffusion of oxygen in the interface resulting in copper oxide CuO formation that happen when copper foil is brought in close contact (under pressure) with alumina plate and heated to a temperature close to its melting point ($1065\text{--}1085 \text{ }^\circ\text{C}$). This oxide becomes chemically bonded with ceramics and forms an intermediate compound—aluminum-copper spinel: $\text{CuO} + \text{Al}_2\text{O}_3 = \text{CuAl}_2\text{O}_4$ [7,18]. The resulting layers have good adhesion and thermal stability. However, DBC process is technologically complex, labor- and time-consuming. For uniform bonding, the copper surface should be acid-etched, and the ceramic surface should be sandblasted. During the bonding process (including heating and cooling stages), copper foil must be pressed to ceramic substrate uniformly over its entire area with large force. In turn, cooling should be gradual (not faster than $\sim 5 \text{ }^\circ\text{C}/\text{min}$, down to $60 \text{ }^\circ\text{C}$), because due to the difference in CLTE, copper exfoliation is possible if cooled rapidly. Thus, despite its prevalence in production,

DBC method requires high temperature of the process coupled with high exerted force in the lamination stage. These conditions are far from being universally tolerable for all ceramic materials that can be utilized in PCB and/or packaging production. Additionally, DBC is naturally only suitable for flat 2D substrates, and cannot be applied when 3D features are present, especially for metallizing 3D structures of ceramic packaging and ceramic PCBs containing through holes.

LTCC/HTCC is based on application to a dielectric and subsequent firing of a special conductive paste consisting of finely dispersed copper powder and an organic binder [12]. The advantage of these techniques is the production flexibility since the paste can be applied in any pattern. However, there are significant drawbacks. Low density of the copper layer reduces electrical and thermal conductivity as compared to the rest of methods mentioned above. The layers demonstrate poor resistance to high temperature, chemicals and moisture, and their physical properties tend to be inhomogeneous. Moreover, thick film technology is resource intensive, since the layer thickness prepared in a single run is limited. In order to build the coating with required thickness, one has to apply the paste several times in a row. After each pass, the paste needs to be dried so that it does not spread. The stability and reproducibility of the layer parameters are also extremely sensitive to the composition of the paste and the firing conditions, which adds to the overall complexity and cost of the process.

Thin film methods, including PVD and plasma-assisted PVD, have low production rate and are rarely used in industrial-scale metallization processes. However, they can be advantageous when we consider substrates with complex shapes and/or situations when applying DBC method is not possible due to thermal and/or mechanical limitations of ceramic material that we need to metalize. In certain cases, PVD methods might outperform more popular industrial-scale technologies in terms of quality and productivity.

Recently, a number of studies were made to introduce new approaches in ceramic metallization. For example, thermal spraying process reported in [16] and its modification of cold gas spraying [17] enables deposition of thick coatings of various materials including metals. The method shows high deposition rate; however, sprayed particles have essentially isotropic distribution of directions, and covering 3D-shaped substrates is therefore complicated. In [9], low-temperature electrochemical ceramic metallization method was studied as an alternative to LTCC and DBC techniques. However, this method requires post-processing of metallized surfaces with laser engraving to form needed metallic patterns. In [11], an alternative method of using liquid copper for wetting of alumina substrate enhanced with Fe_2O_3 powders was studied. In this case, an additional step of Fe layer sintering is needed. Additionally, laser irradiation stage is used to create fine crevice structure on metallized surface suitable for filling it with liquid tin, for subsequent joining with other parts.

Therefore, despite having production-scale DBC and LTCC techniques, development of new approaches continues and results in a diverse selection of methods that have specific advantages and can be applied in those cases when more universal DBC and LTCC are not effective or optimal.

In this work, we studied the possibility of using magnetron discharges of various types (with cooled and heat-insulated (hot) targets) for metallization of alumina ceramic substrates with copper coatings. One of the main goals was to metallize complex-shaped substrates, in particular, to deposit copper on faces situated under steep angles with respect to the surface normal and on surface features whose height is comparable with coating thickness. The possibility of complete covering of PCB with through holes was studied as well. The adhesive properties of metallizing layers were studied, and the way of their improvement by introducing intermediate copper oxide layer was tested.

2. Experimental Methods

2.1. Experimental Setup

Magnetron deposition of copper on alumina ceramic was studied in the experiments in two setups: conventional confocal magnetron sputtering setup with a cooled-target magnetron, and a custom setup where the magnetron is equipped with a thermally insulated target [19,20].

Confocal magnetron sputtering setup scheme is shown in Figure 1. A single slightly unbalanced circular magnetron (Magneto series by Pinch, LLC, Moscow, Russia) was used out of three available in the installation. Sputtering was performed from a 76.2-mm-diameter copper target with 99.999% purity (Goodwill Metal Tech Co., Ltd., Beijing, China). The samples were placed on a rotating stage in front of the magnetron target, at a distance of 8 cm. The uniform deposition without shadowing effects was realized by tilting the magnetron with respect to the sample surface plane and rotating the sample stage with a speed of 1.5 rpm. During the deposition, a constant bias voltage of -100 V was applied to the sample stage.

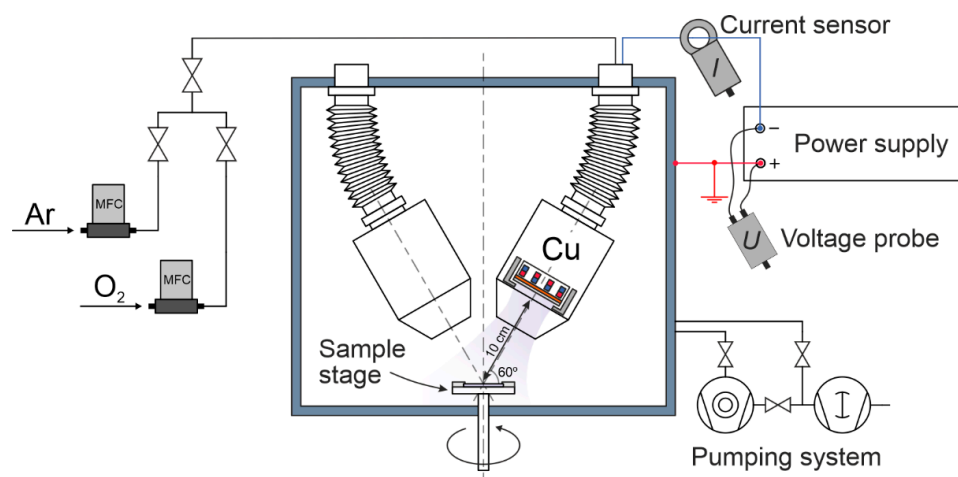


Figure 1. Conventional magnetron sputtering system with a cooled target.

The vacuum chamber was pumped down to a base pressure of 10^{-4} Pa with a turbomolecular pump backed by a multi-stage dry Roots pump. The working gases (argon, oxygen, and their mixtures) were supplied by automated mass-flow controllers El-Flow (Bronkhorst High-Tech B.V., AK Ruurlo, The Netherlands). DC discharge power supply APEL-M-5PDC-800 (Applied Electronics, LLC, Tomsk, Russia) was operated in the range 500–1500 W. Working gas pressure was 1 Pa.

Copper deposition time was up to 60 min. At the end of the deposition, the samples were cooled for 15 min in argon atmosphere.

In the experiments with copper oxide deposition, the composition of the working gas and the discharge power were varied according to the following scenario. First, to deposit an oxide sublayer, argon and oxygen were introduced into the chamber in various proportions at low discharge power (<500 W). After a certain time period (required for deposition of copper oxide film with necessary thickness), the oxygen supply was turned off, and the discharge power was increased to 1500 W to accelerate the deposition of the main (bulk) copper layer. The deposition time for bulk copper layer was ~ 40 min. The deposition rate of the CuO coating was ~ 0.5 $\mu\text{m}/\text{min}$, and that of the main Cu coating was ~ 0.8 $\mu\text{m}/\text{min}$.

Due to the high power of the magnetron discharge, it was necessary to provide sufficient cooling in order to avoid unwanted overheating of the target. For better heat removal, a thermal grease interface was applied between the target and the cathode.

Scheme of the custom setup with hot-target magnetron is shown in Figure 2. Here, the magnetron has a thermally insulated target with a diameter of 98 mm. Copper target was placed in a special molybdenum crucible resting on a set of miniature tungsten support

legs. A heat shield was placed around the target. On top of it, the heat shield had a substrate-sized opening. Since the coating deposition rate in such system can be as high as tens of $\mu\text{m}/\text{min}$ [19–21], a mechanical shutter was used to open/close this opening. It was a means to separate the magnetron discharge area from the remaining part of vacuum chamber. Hence, the shield not only acted as a thermal screen, but also prevented the target material flux from escaping the discharge region and depositing on the substrate.

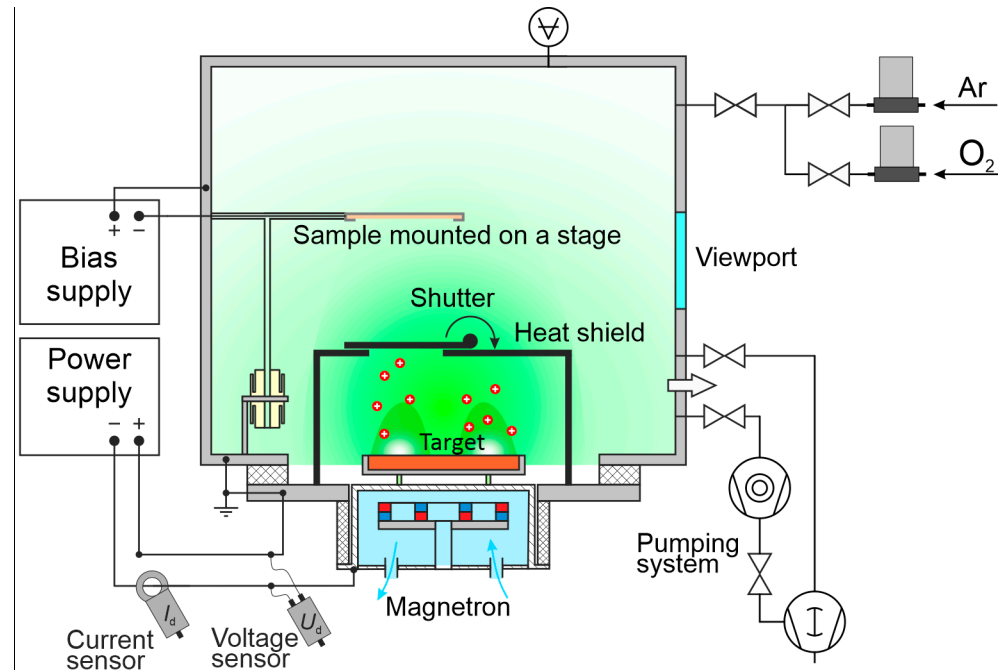


Figure 2. Hot-target magnetron deposition setup.

The vacuum chamber was pumped down to a base pressure of 10^{-4} Pa with a turbomolecular pump backed by a multi-stage dry Roots pump. The working gases (argon, oxygen, and their mixtures) were supplied by automated mass-flow controllers El-Flow (Bronkhorst High-Tech B.V., AK Ruurlo, The Netherlands). DC discharge power supply APEL-M-5PDC-800 (Applied Electronics, LLC, Tomsk, Russia) was operated in the range 500–3000 W.

When using a hot-target magnetron for copper coating deposition, its material was at first preheated with a 1500 W discharge at an argon pressure of 1 Pa. After copper target melted, once thermal equilibrium was established and the operating parameters demonstrated stabilization, the argon gas inlet was closed, and the discharge was maintained exclusively in copper vapor [20]. In order to increase film uniformity and more accurately control the thickness of deposited copper, the shutter was kept closed from the moment of turning the power supply on until establishing thermal equilibrium. At this point, when the evaporated and sputtered fluxes were stabilized and the working gas inlet was closed, the shutter was opened for the deposition period. After that, the shutter was closed again to prevent the evaporated copper atoms from reaching the sample. In the end, the sample was cooled in an argon atmosphere at a pressure of ~ 100 Pa for about 30 min.

In the experiments with copper oxide deposition, the first process stage was sputtering of solid copper target at low power (200–300 W) in an argon-oxygen environment in order to create an intermediate Cu_xO_y layer, the same way as in the conventional sputtering system described above. Afterwards, the shutter was closed, the oxygen flow was set zero, and the discharge power was increased. After the copper melted and stabilizing of discharge parameters, the shutter was opened, and the main copper layer was deposited on the substrate. A bias voltage of -100 V was applied to the sample stage.

2.2. Advantages of Hot-Target Magnetrons

Conventional magnetron sputtering with a cooled target has an intrinsic drawback of low energy efficiency (<5%), since most of the discharge power is dissipated in the radiative form, while heat is removed by the target cooling system and is not used further. From this point of view, hot-target magnetrons are advantageous since they offer combination of ion sputtering and evaporation. Deposition rate in a hot-target magnetron can be 10–100 times higher than that in a classical one at the same power [19–21]. Magnetron operation in gasless self-sputtering mode eliminates influence of working gas atoms and ions on the properties and structure of prepared films [22]. Additionally, for melted targets, the amount of utilized material can be up to 100%, and it can be easily refilled in the crucible.

Figure 3 shows mass spectra of the ion flux from magnetron plasma to the substrate area for a cooled (Figure 3a) and a hot copper target magnetron in gasless mode (Figure 3b).

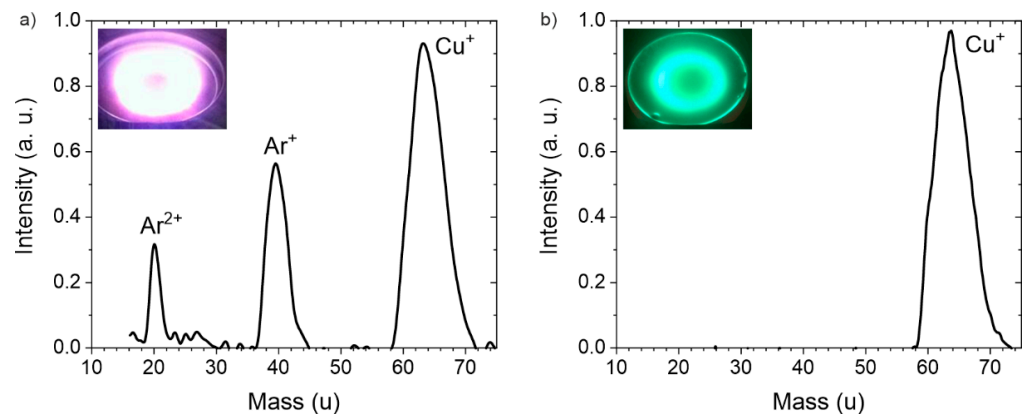


Figure 3. Mass spectra of ion flux in the substrate area: (a) magnetron with a cooled copper target; (b) magnetron with a hot copper target in gasless self-sputtering mode.

Using the gasless self-sputtering mode improves the purity of the deposited copper layer, since in classical systems there are always non-zero fractions of gas ions and atoms that are introduced into the surface of the film from plasma and become incorporated in the film during its growth.

In hot-target magnetrons, the flux of evaporated atoms facilitates film growth in a way similar to the thermal evaporation method. Thus, total flux of particles deposited on the substrate consists of comparatively high-energy (up to 10 eV) sputtered atoms and low energy (thermal, ~0.1 eV) evaporated ones. In many cases, this combination is beneficial for production of coatings since it brings together high deposition rates of thermal evaporation method and high energy of particles associated with classical sputtering.

2.3. Sample Preparation

Alumina substrates (60 mm × 48 mm × 0.5 mm plates, Al₂O₃ 96%, GN Electronics, Moscow, Russia) were prepared by laser cutting and drilling. For some experiments, smaller substrates 24 mm × 15 mm × 0.5 mm were laser-cut from the original plates. All samples were cleaned in an ultrasonic bath with ammoniacal hydrogen peroxide solution.

2.4. Diagnostic Methods

The structure, composition, mechanical, and electrical properties of prepared coatings were analyzed by a number of standard diagnostic methods.

The scanning electron microscopy (SEM) and X-ray energy dispersive spectrometry (EDS) diagnostics were conducted in Vega 3 (Tescan, Brno, Czech Republic) microscope equipped with X-Act spectrometer (Oxford Instruments, Abingdon, UK). The thickness of the prepared coatings and the roughness of the samples were determined with Dektak 150 (Veeco, Tucson, AZ, USA) surface profiler. Adhesion of coatings was investigated by Anton Paar Revetest scratch-tester. The X-ray diffractometry (XRD) diagnostic was conducted

with DRON-3 automated double-crystal diffractometer (IC Bourestnik, Saint-Petersburg, Russia) operating in the Bragg-Brentano scheme using quartz monochromator and Cu $K\alpha$ 1 radiation. The surface resistance R_s of deposited films was measured by a well-known four-probe method in a custom-built setup. The resistivity ρ was then calculated as $\rho = R_s \times h$, where h is the film thickness. The thermal performance tests were made by custom procedures described in Section 3.4.

3. Results

3.1. Preliminary Experiments

Initially, experiments were conducted to test the feasibility of magnetron deposition method for filling through holes and covering the complex-shaped surface features, especially, the faces located at steep angles with respect to surface normal.

Both cooled- and hot-target magnetron deposition methods demonstrated nearly the same ability of filling the through holes. Photograph of a substrate with laser-drilled holes with minimal diameter of 10 μm after copper deposition is shown in Figure 4a. Figure 4b shows SEM images of 80- μm diameter hole coated in cooled target mode and in hot-target evaporative mode together with that of a large 600- μm diameter hole.

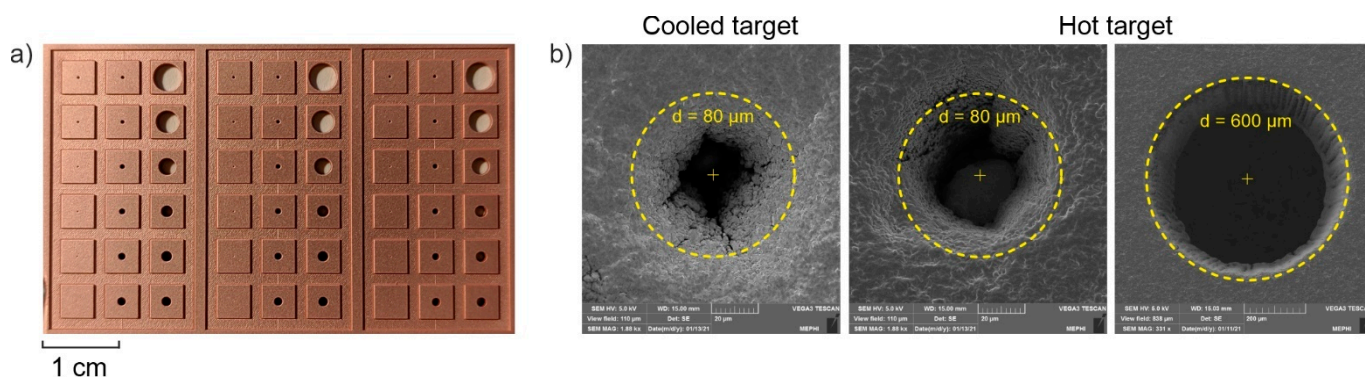


Figure 4. (a) Alumina substrate with laser-drilled through holes covered with copper film; (b) comparison of SEM images of 80- μm diameter through hole with copper coating deposited by cooled and hot-target magnetron sputtering, and SEM image of 600- μm diameter through hole coated in hot-target magnetron mode.

SEM results demonstrate that the deposition in the holes has good continuity, including the hole walls. In both the cooled- and hot-target magnetron modes, copper coatings thicker than 60 μm completely covered 30- μm -diameter through holes. In Figure 4b, images of 80- μm diameter holes are presented since this is the value when coverage starts to be incomplete, and one can have a better look on the coating structure. Discussing the SEM results in Figure 4b, one should also keep in mind the method of initial hole drilling process. Laser machining of holes leaves cone angle of $\sim 5\text{--}10^\circ$. Additionally, the characteristics of CAM laser machining result in non-uniform “wavy” contour of circumference, which can be noticed in all holes. This effect can be clearly observed in Figure 4b in the rightmost image of a 600- μm diameter hole.

Magnetron deposition from cooled target resulted in slightly denser coating structure than in the hot-target mode. Additionally, coatings deposited in the hot-target magnetron at extremely high discharge power contained droplet phase and improving the surface quality in this case required additional treatment. Nevertheless, hot-target mode offers much higher deposition rates.

Despite good film structure and deposition rates, the coating adhesion was poor for thick (>50 μm) films. We observed delamination of films after weak mechanical impact. Since metallization requires more than 50–100 μm copper thickness, the parameters of adhesion and coating resistance to thermal and mechanical effects are extremely important. However, standard diagnostic techniques are as a rule not suitable for the complex-shaped

samples. Therefore, the second step was to test the process of deposition of relatively thick copper coatings with simple planar geometry on alumina substrates.

To provide statistical representation, we prepared Cu films in the pattern of several tens of isolated island areas. This was done in two ways. The first one was the deposition of copper inside an array of laser-engraved cavities in planar alumina substrate. The bottom surfaces of cavities were textured with laser and had larger roughness than the initial alumina substrate. The results of deposition are shown in Figure 5a. The second method was to deposit copper on a planar alumina substrate through a shadow mask with an array of rectangular openings. The results are shown in Figure 5b.

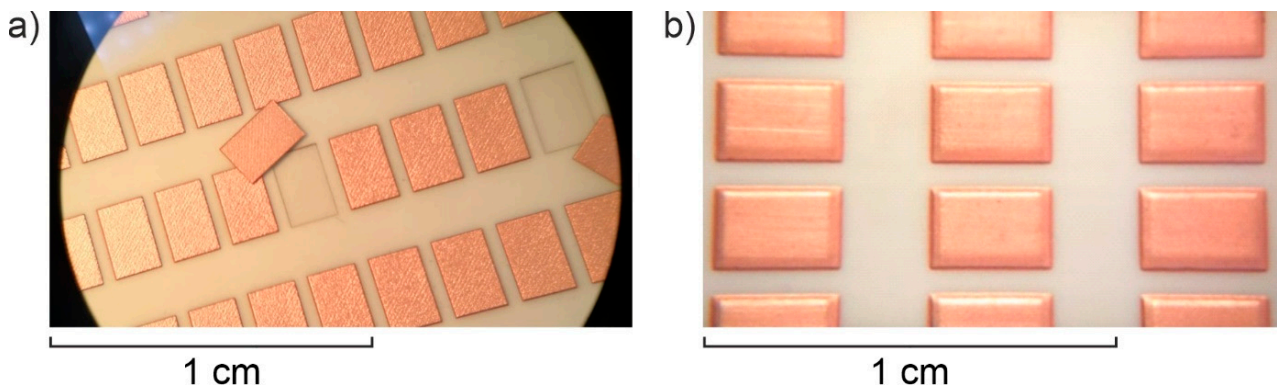


Figure 5. Images of copper film deposited on alumina substrate: (a) in the laser-engraved cavities; (b) on a planar substrate through a shadow mask.

On the sample with cavities, several islands delaminated immediately. The rest of the islands had poor adhesion as well and could not resist the mechanical impact. The increase in roughness did not improve the adhesion.

The islands deposited through rectangular mask performed much better. The samples did not delaminate after mechanical impact. The total thickness of coating was $\sim 120 \mu\text{m}$. The surface roughness was the same as of the original substrate ($R_a = 0.2\text{--}0.7$).

To study the coating structure, the substrate was laser-cut, and the cross-section was investigated in SEM. The SEM image of the island and substrate cross-section is shown in Figure 6a. A closer image of the interface is shown in Figure 6b.

Propagation of a crack is clearly visible in the interface region. Probably it originated from heat shock during the laser cutting of the sample. However, the following $20\text{--}250 \text{ }^\circ\text{C}$ thermal cycling led to copper delamination from regions outside the cutting edge area after ~ 10 cycles (see Figure 6c). Thermal cycling therefore results in formation and/or development of such cracks that stimulate delamination process. Thickness of the copper islands was $100\text{--}120 \mu\text{m}$.

For thicker coatings, the situation is worse. Due to the difference in the CLTE of the connected materials, numerous thermal cycles or overheating result in occurrence and development of mechanical stresses in the substrate/coating interface. It can result in cracking in the boundary layer, reduction in heat removal ability, and in the end, in detachment of the copper layer from the ceramic substrate.

To improve the adhesion of copper to ceramics and, thereby, extend the service life of a PCB or packaging, the use of intermediate compensation layers might help. Such layers should be designed to absorb stresses that evolve in the interface as a result of temperature fluctuations, hence improving the adhesion.

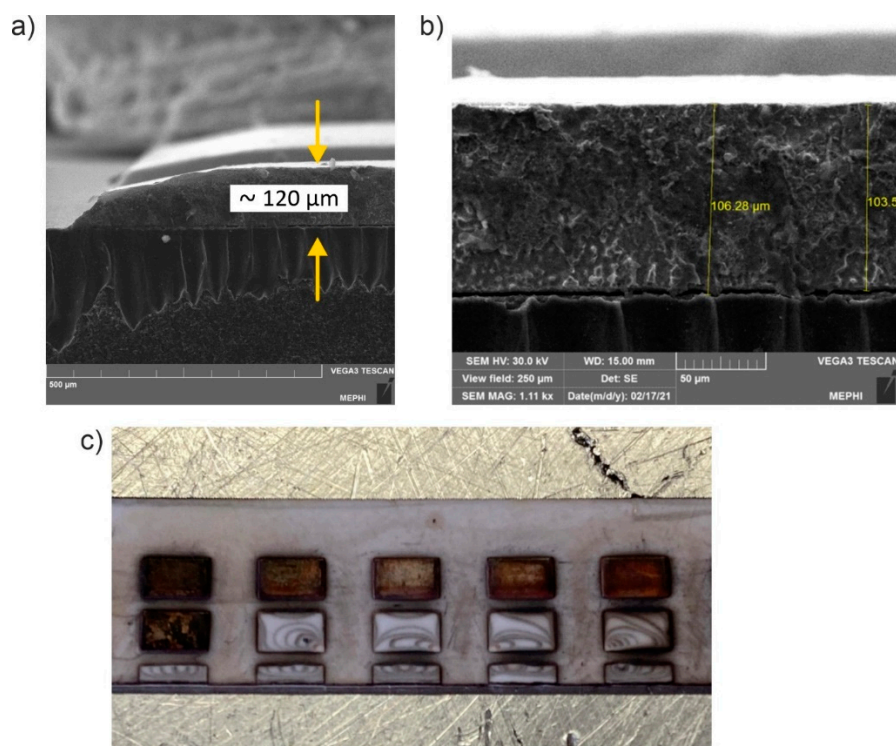


Figure 6. Copper film deposited on alumina substrate through a shadow mask: (a) SEM image of Cu island cross-section; (b) SEM image of the interface; (c) sample from Figure 5b after thermal tests.

3.2. Two-Layer Coating

A number of options is known to produce various compensating intermediate layers to increase the adhesion between the substrate and the coating. In our case, copper oxide can be considered as an intermediate layer, since it does not introduce materials other than those already present in Cu/Al₂O₃ system and has suitable mechanical and thermal properties. In magnetron sputtering systems, such a sublayer can be prepared in a continuous process with metallization, without adding complex technological operations. In this case, copper is reactively sputtered in an argon–oxygen mixture. Copper is easily oxidized at elevated temperatures (>200 °C), which can be readily achieved in a magnetron discharge. When oxygen is added to the working gas mixture, it interacts with the heated copper layer, and an oxide Cu_xO_y is formed. Exact stoichiometry and layer thickness of Cu_xO_y film are determined by the experimental parameters.

It is assumed that in this case, similar to the situation in the DBC method, a very thin eutectic bond should form between alumina and copper oxide due to higher-energy particles bombarding the surface. Stimulating chemical reaction $\text{CuO} + \text{Al}_2\text{O}_3 = \text{CuAl}_2\text{O}_4$ similar to that in DBC requires obtaining a stoichiometric copper oxide, namely, CuO. In the process of magnetron deposition, the stoichiometry of the coating can be varied by changing the fraction of oxygen in the working gas [23,24]. It also depends on other factors, including discharge power, deposition rate, substrate, and target temperature. Coating thickness can be easily controlled by the time of copper sputtering in an argon–oxygen mixture. In [24], the dependence of the fraction of stoichiometric copper oxides constituting a film deposited in a DC magnetron discharge on the oxygen/argon ratio in the working gas mixture was experimentally studied. Predominant growth of stoichiometric CuO in [24] was done with an oxygen-to-argon ratio of 40/60. Keeping this result in mind, we conducted experiments with changing the reactive gas mixture during Cu_xO_y sublayer deposition. However, in our work, the quality of the metallization could be assessed only by testing the adhesion of a resulting two-layer film. It was not possible to perform individual diagnostics of a Cu_xO_y sublayer within the compound coating. Therefore, Cu_xO_y sublayer properties

were investigated in a separate set of experiments, and their results are reported later in Section 3.5.

Preliminary diagnostics were done according to the following scheme. At first, Cu_xO_y layer was deposited on alumina substrate. The thick Cu layer was deposited in vacuo right onto the sublayer. This enabled express testing of Cu_xO_y ability to improve adhesion by investigating the performance of the coating as a whole.

After preliminary tests, we selected optimal regimes for sample preparation. Smaller substrates $24 \text{ mm} \times 15 \text{ mm} \times 0.5 \text{ mm}$ were used for the $\text{Cu}_x\text{O}_y + \text{Cu}$ depositions as they were required for scratch-testing and XRD studies.

Figure 7 shows the profiles of the coating substrate steps formed during the deposition of CuO coating and composite CuO + Cu film. A special alumina shadow mask was used to prepare coating steps suitable for profilometry.

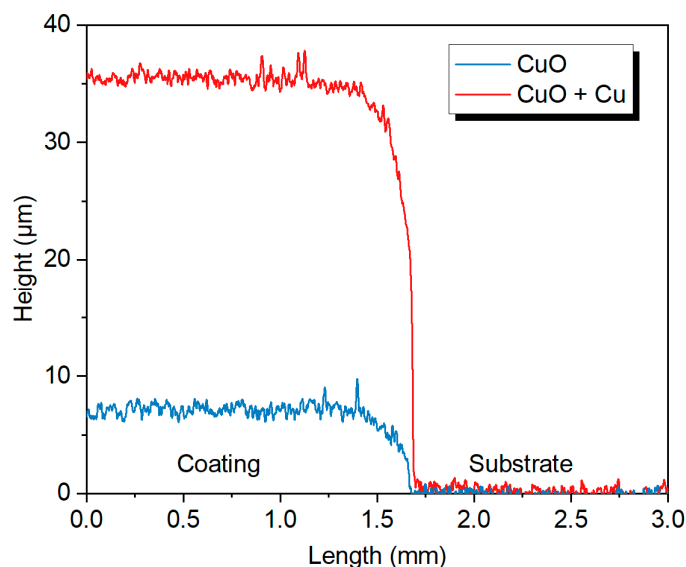


Figure 7. Surface profile of a thick Cu coating and of a CuO intermediate layer (measured separately).

Samples prepared in this way exhibited good adhesion and were visually of good quality. It can be seen from the surface profile that the roughness of the resulting layer is close to that of the initial substrate (in this particular case $R_a \sim 0.3 \mu\text{m}$). Therefore, there are no defects or droplets, and the coating thickness is uniform.

Thickness of copper oxide sublayer was found to influence the performance of two-layer coating. Since we did not study the sublayer thickness beforehand, the optimal thickness value was chosen empirically. For this purpose, we varied deposition time for oxide layer, while the time of main copper layer deposition was fixed. Analogously to choosing the right Cu_xO_y stoichiometry, optimization was conducted by changing the deposition time parameter and testing the performance of compound $\text{Cu}_x\text{O}_y + \text{Cu}$ coating. Detailed study of copper oxide sublayer properties including its thickness was made separately and is reported in Section 3.5.

Thickness of the two-layer coatings was in the range 35–40 μm (together with the sublayer). From separate experiments, optimal copper oxide film deposition parameters were determined. With these parameters, Cu_xO_y ($x = 1, y = 1$) film was deposited separately with the same shadow mask, and its profile was measured. It is shown in Figure 7 together with the total CuO + Cu coating thickness profile. The optimal value of CuO thickness was found to be 5–7 μm .

The electrical resistivity of the prepared coatings was estimated by the four-probe method. For all samples, $\rho \approx 1.7 \times 10^{-8} \Omega \times \text{m}$, which corresponds to the reference data for resistivity of pure copper. Thus, the layer prepared on alumina substrate had strong metallic properties.

3.3. Scratch-Testing

For a more accurate assessment of the quality and adhesion of the applied layer, scratch testing of the copper layers on the obtained samples was conducted. A Rockwell diamond type indenter with a tip radius of 200 μm was used. The load was linearly increased from 0.3 to 20 N. Scratch length was 5 mm. Feed velocity was 2.54 mm/min, and force increase rate was 10 N/min. The results are shown in Figure 8.

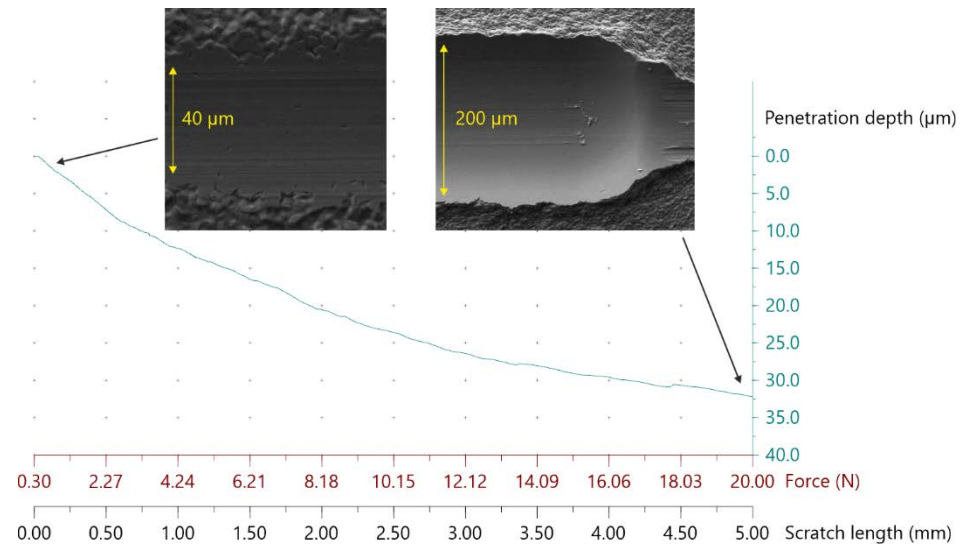


Figure 8. Scratch-testing results: penetration depth vs. exerted indenter force together with SEM images of scratch ends.

SEM images of the beginning and the end of a scratch indicate good uniformity of the indenter track, without delamination or cracking of the film. The plot of the penetration depth versus the indenter path coordinate has an almost monotonic and smooth shape. This also indicates the absence of defects and good uniformity of the film thickness. The absence of acoustic signal peaks at a full run of the indenter over the copper film means that no cracking or delamination occurred during penetration, which also indicates high quality of the resulting layer. In the range of 0.3–20 N test load, the indenter penetrated the surface down to a depth equal to the coating thickness. The film remained undamaged and did not exfoliate.

Thus, application of a thick copper coating onto copper oxide sublayer results in excellent adhesion of metallizing coating.

3.4. Thermal Tests

Thermal cycling of produced coating was conducted by rapid increasing sample temperature from 25 $^{\circ}\text{C}$ to 600 $^{\circ}\text{C}$, then slow decreasing it down to 25 $^{\circ}\text{C}$. Figure 9 shows a sample after the scratch test and the same one prepared for thermal cycling. To reduce sample oxidizing and damaging, we covered samples with solder.

Tests were conducted by simulating extreme conditions for electronic devices. For this purpose, a temperature-controlled soldering bath was used. Adhesion was estimated by the number of cycles until the copper layer delaminates from the ceramic substrate.

One cycle consisted in keeping the samples first in the solder bath (without tin), then in air for about 2–3 min, so that the whole cycle does not exceed 5 min. The time periods of heating and cooling were experimentally selected so that the sample had time to heat up approximately to the temperature of the bath. The temperature of the solder bath was varied in the range of 250–400 $^{\circ}\text{C}$.

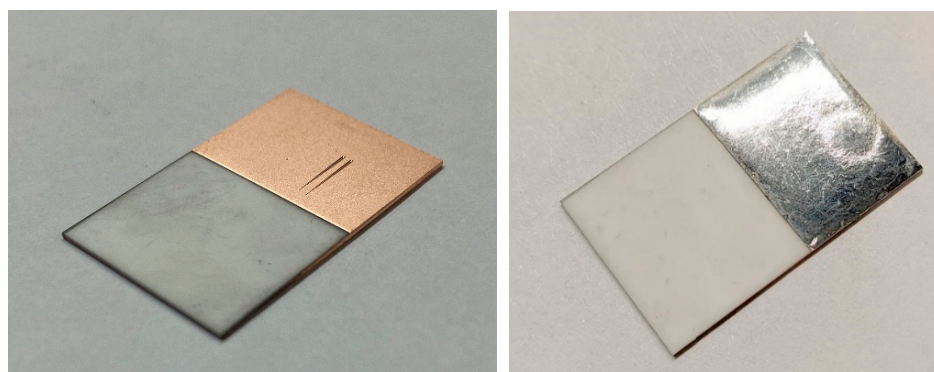


Figure 9. Photographs of prepared CuO + Cu coating after scratch testing and after soldering.

Then, the thermal cycling was conducted in tin bath. In this case, the coatings were damaged more intensively due to large thermal conductivity of tin. This resulted in high heating rate of the surface and corresponding extremely steep gradient of temperature in the interface area. Such conditions facilitate formation of cracks and defects.

The optimized coatings withstood 130 thermal cycles in air. Next, they were dipped into molten tin at a temperature of 350–400 °C. The coating with sublayer withstood seven immersions, after which the ceramic substrate cracked. The coating without the sublayer was destroyed in the very first cycle in molten tin.

In a separate test, a copper wire was successfully soldered to one of the samples, and no delamination of the copper layer was observed.

3.5. Intermediate Oxide Layer

It was not possible to study the properties of oxide layers after the deposition of main copper coatings. A dedicated series of experiments was conducted in conventional cooled-target magnetron. It was aimed at studying the mechanism of improving the adhesion of thick copper layers by preliminary reactive deposition of copper oxide used as a sublayer. For the experiments, we used the same conditions as in $\text{Cu}_x\text{O}_y + \text{Cu}$ depositions.

First, the deposition of oxide without the main copper layer was tested to check the stoichiometry depending on the fraction of oxygen in the reactive working gas mixture in a way similar to that in [24]. Diagnostics of the resulting oxide films by EDS and XRD analysis were made for selected samples deposited at oxygen-to-argon ratios 40/60 and 30/70, since corresponding $\text{Cu}_x\text{O}_y + \text{Cu}$ metallization coatings showed superior properties as compared to other reactive gas mixtures. Table 1 contains EDS data for selected Cu_xO_y samples.

Table 1. EDS data for copper oxide intermediate layers.

Sample No.	O ₂ /Ar Gas Ratio	Cu Fraction in Film	O Fraction in Film	Cu/O Ratio in Film	Compound
1	30/70	66.8%	32.7%	~2	Cu ₂ O
2	40/60	42.4%	48.8%	~0.9	CuO

EDS spectra demonstrate preparation of two types of stoichiometric oxides: Cu₂O and CuO. Transition between fully and partially oxidized copper occurs between 40/60 and 30/70 O₂/Ar gas ratio values.

XRD diffractograms of coatings are shown in Figure 10. Peaks were identified according to Crystallography Open Database (COD): Cu₂O (COD entry 9007497), Al₂O₃ (COD entry 1000017).

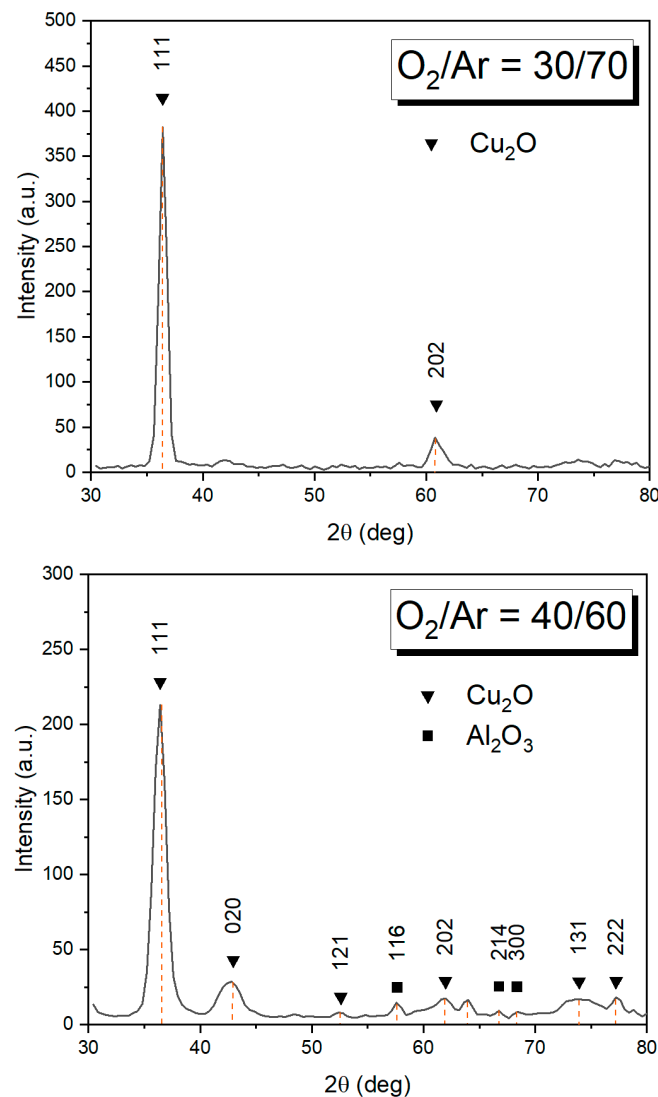


Figure 10. XRD diffractograms of copper oxide sublayer films.

Unfortunately, we cannot deduce quantitative data from recorded XRD diffractograms. In general, higher intensity should indicate larger amount of corresponding phase in the film. However, different phases might constitute different sizes of crystallites, and, in this case, the estimation of their relative abundance by peak intensities would be incorrect.

In Figure 10, intensity of XRD peaks is comparatively low that suggests fine crystalline structure, which is almost isotropic. From EDS we expect to observe CuO and Cu_2O crystallites; however, XRD diffractograms show only Cu_2O peaks. This dissonance is associated with specific features of film growth process on alumina substrate and our experimental conditions. For $O_2/Ar = 30/70$ case, larger Cu_2O crystals are formed, while the rest remains non-detectable for XRD. Presumably, these Cu_2O crystals are surrounded by dominating amount of fine CuO grains. In $O_2/Ar = 40/60$ case we observe more complex texture that contains peaks corresponding to differently oriented crystallites.

Combining EDS results with XRD results, we conclude that fine-grain polycrystalline Cu_xO_y was prepared. However, at $O_2/Ar = 30/70$ gas ratio, Cu/O ratio in the film was about 2. For $O_2/Ar = 40/60$ gas ratio, oxygen in the films is presumably distributed in the amorphous form or is located outside the crystals due to its high solubility.

Comparing our results with those known for DBC, we agree that copper oxide is beneficial for producing intermediate layer that improves the adhesion of main Cu coating to Al_2O_3 substrate. However, in our experiments both CuO and Cu_2O sublayers show positive effect on the performance of resulting metallizing coating.

Thickness of copper oxide films was optimized to prevent delamination of CuO + Cu coatings thicker than 20 μm . First, a sublayer thickness of 10–15 μm was chosen, on top of which the main copper layer with ~ 30 μm thickness was deposited. However, the coatings exfoliated immediately after cooling. Consequently, the thickness of the sublayer was reduced and in the final experiments was about 5–7 μm .

3.6. Summary of Coating Properties

By combining the diagnostic results obtained for two-layer Cu_xO_y + Cu coatings and separately measured characteristics of intermediate Cu_xO_y layers, we can summarize quantitative information related to the coatings that match the requirements for alumina metallization in production of ceramic PCBs or packaging. The results are presented in Table 2.

Table 2. Overview of properties of composite Cu_xO_y + Cu metallizing coatings.

Property	Value
Resistivity ρ ($\Omega \times \text{m}$)	1.7×10^{-8}
Roughness Ra (μm)	0.3
Cu thickness (μm)	30–120
Cu/O ratio	0.9 or 2
CuO thickness (μm)	5–7

4. Discussion

The proposed method of applying comparatively thick (>100 μm) metallizing coating proved its feasibility. The quality of coatings prepared in hot-target magnetron with the sublayer is better than without it, but worse than in cooled-target magnetron with the sublayer. Cooled- and hot-target magnetron deposited Cu coatings without the Cu_xO_y sublayer are almost the same, except droplets are formed in the hot-target process at extremely high values of discharge power.

Plasma PVD deposition of intermediate layer is characterized by the substrate bombardment with energetic particles (ions and sputtered atoms) that contributes to surface monolayer interface mixing between Cu/ Cu_xO_y and $\text{Cu}_x\text{O}_y/\text{Al}_2\text{O}_3$. Hence, presence of energetic particles enables improving the coating adhesion without the need for extreme conditions (high temperature and/or large compressive force), which are required for current industrial scale processes, such as DBC and LTCC.

Additionally, we demonstrated that PVD deposition allows effectively metallizing the complex shaped surface features including those having faces under steep angles to surface normal, which is problematic for conventional DBC method.

For prospective development of PVD methods, we suggest a technique of preparing metallizing films using magnetron sputtering and evaporation modes. The structure of a resulting coating is shown in Figure 11.

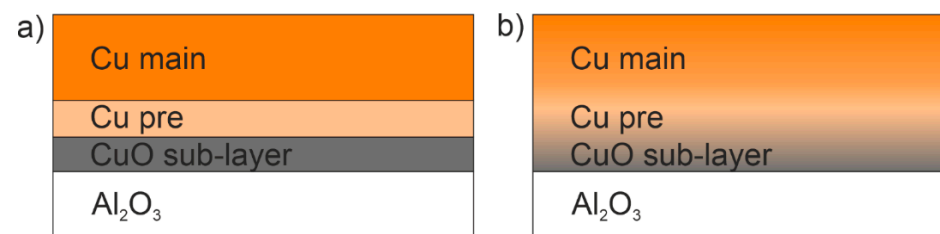


Figure 11. (a) Structure of a multi-layer metallizing film; (b) Structure of a gradient metallizing film.

The coating should consist of following layers and could be prepared as follows. At first, copper oxide sublayer should be deposited in well-controlled conditions. This can be effectively done in a cooled-target magnetron [25]. Then, a thin dense “Cu pre coating” should be applied. Here, plasma with higher concentration is required to produce larger

ion flux on the substrate, and, thus, enhance the film density. Cooled-target magnetron in this case can be operated in the high-power impulse magnetron sputtering (HiPIMS) mode. In a hot-target magnetron discharge, which is known to enhance plasma density near the substrate [20], the coating density is lower. The main metallizing layer can be prepared as a thick and not-so-dense Cu coating. Since thickness about hundreds of μm is excessive for the cooled-target magnetrons, very high-rate process is required here, e. g. hot-target magnetron, thermal evaporation, or galvanic deposition (electroplating). Excellent adhesion between copper layers with different density does not require energetic particle bombardment or any particular chemical bonding. Hot target magnetron deposition in this case would act as a lamination stage.

It is worth noting that a hot-target magnetron in HiPIMS mode [26] could virtually be suitable for realizing all described stages in a single run. By starting the magnetron discharge in oxygen atmosphere, gradually increasing power, decreasing oxygen flow, and, finally, entering gasless self-sputtering mode with liquid copper target, the gradient coating structure as in Figure 11b can be realized in a single continuous process. The interface CuO–Al₂O₃ region in this case should stimulate oxygen diffusion between substrate and coating and improve the adhesion in a way similar to DBC method.

We expect that applying HiPIMS modes to hot-target magnetron would improve the stability of Cu_xO_y deposition and increase its deposition rate as compared to a cooled target magnetron.

Hot-target magnetron operation with liquid copper target is well studied both in DC and HiPIMS modes [20,21,26]. For its further application, it is necessary to investigate the processes of creating intermediate compensation layers. Therefore, subsequent experiments are needed to study the processes of hot-target reactive deposition of copper oxide coatings to increase the deposition rate and make the technology more stable and controllable.

When comparing methods of magnetron deposition with hot and cooled targets and DBC technology, in addition to some of the indicated drawbacks of magnetrons, their significant advantages should also be noted. In both methods, the adhesion depends on the sublayer thickness. From this point of view, magnetron methods are beneficial, since when applying a sublayer, as described above, the thickness can be easily controlled by the time of copper deposition with oxygen admixture in the working gas. In its turn, DBC does not provide a way for thickness adjustment. Another issue is regulating the quality of DBC layers, since the amount of oxygen decreases during metallization, and in some cavities, it may not be enough to form the required oxide. In magnetron deposition method, oxide is continuously grown during the sputtering process, and the oxygen fraction is constant. In [18], a method of preliminary magnetron deposition of copper oxide onto copper foil was proposed prior to DBC lamination. The sample obtained by this method had wider and more uniform ceramic–copper interface. This indicates a possible better behavior in real applications.

For the formation of a homogeneous high-quality connection, close microscopically tight contact between copper foil and ceramic is necessary. For these purposes, the surfaces must be carefully processed and comply with tough roughness requirements. The foil itself must be kept near the melting point during the joining process so that the molten copper could wet and replicate the surface of the ceramic plate. In magnetron sputtering, the layer grows directly on the ceramic surface, thus, these issues are irrelevant. Notable advantages of the magnetron method compared to DBC include the possibility of applying coatings to geometrically complex samples (multi-level, with vias, through holes, etc.). There is also the possibility of tuning the adhesion of copper by changing the magnetron deposition parameters.

We believe that combining different magnetron deposition modes in a single process or in a number of in vacuo processes can outperform DBC regarding the ability to metallize geometrically complex objects. It enables metallization of (laser) machined ceramic components (PCBs or packaging) in any patterns.

5. Conclusions

- A series of experiments on the metallization of alumina ceramics with copper in magnetrons with a hot/liquid and cooled target under different conditions and deposition parameters have been conducted.
- It has been shown that magnetron deposition is suitable for preparing thick (>100 µm) low-resistivity metallizing copper layers, including those in through holes and those deposited through shadow masks. However, direct copper deposition on alumina does not yield coatings resistant to thermal and mechanical loads.
- Optimal conditions for creating compensation CuO and Cu₂O sublayers that improve the adhesion of thick (>35 µm) composite Cu_xO_y + Cu coatings have been obtained.
- CuO + Cu composite coatings demonstrated best stability in thermal cycling tests.
- An approach of fully in vacuo magnetron deposition process for preparation of a multilayer metalizing coating on alumina is proposed that is beneficial for processing ceramic PCBs or packaging with complex geometry.

Author Contributions: Methodology, K.Y.O.; Investigation, V.Y.L., A.V.T. and M.M.K.; Resources, K.Y.O.; Writing—original draft, A.V.T.; Writing—review & editing, A.V.K. and D.V.K.; Project administration, A.V.K. and N.N.S. All authors have read and agreed to the published version of the manuscript.

Funding: This research was funded by the Russian Science Foundation (Grant No. 18-79-10242).

Institutional Review Board Statement: Not applicable.

Informed Consent Statement: Not applicable.

Data Availability Statement: The authors confirm that the data supporting the findings of this study are available within the article.

Acknowledgments: The authors are grateful to T.V. Stepanova for performing the scratch-tests.

Conflicts of Interest: The authors declare no conflict of interest.

References

1. Samotaev, N.; Oblov, K.; Dzhumaev, P.; Fritsch, M.; Mosch, S.; Vinnichenko, M.; Trofimenko, N.; Baumgärtner, C.; Fuchs, F.M.; Wissmeier, L. Combination of Ceramic Laser Micromachining and Printed Technology as a Way for Rapid Prototyping Semiconductor Gas Sensors. *Micromachines* **2021**, *12*, 1440. [[CrossRef](#)]
2. Fritsch, M.; Mosch, S.; Vinnichenko, M.; Trofimenko, N.; Kusnezoff, M.; Fuchs, F.M.; Wissmeier, L.; Samotaev, N.; Etrekova, M.; Filipchuk, D. Printed Miniaturized Platinum Heater on Ultra-Thin Ceramic Membrane for MOX Gas Sensors. *Springer Proc. Phys.* **2021**, *255*, 97–103. [[CrossRef](#)]
3. Samotaev, N.N.; Oblov, K.Y.; Gorshkova, A.V.; Ivanova, A.V.; Philipchuk, D.V. Ceramic Packages Prototyping for Electronic Components by Using Laser Micromilling Technology. *J. Phys. Conf. Ser.* **2020**, *1686*, 012010. [[CrossRef](#)]
4. Dusek, K.; Busek, D.; Hrzina, P.; Sevcik, J. Thermal Cycle Testing of Printed Circuit Board Vias (Barrel Plates). *Proc. Int. Spring Semin. Electron. Technol.* **2018**, *2018*, 3608. [[CrossRef](#)]
5. Zhang, S.; Yan, L.; Gao, K.; Yang, H.; Yang, L.; Wang, Y.; Wan, X. Thermal Ratchetting Effect of AMB-AlN Ceramic Substrate: Experiments and Calculations. *Ceram. Int.* **2019**, *45*, 14669–14674. [[CrossRef](#)]
6. Liu, B.; Sha, K.; Zhou, M.F.; Song, K.X.; Huang, Y.H.; Hu, C.C. Novel Low-Er MGa₂O₄ (M = Ca, Sr) Microwave Dielectric Ceramics for 5 G Antenna Applications at the Sub-6 GHz Band. *J. Eur. Ceram. Soc.* **2021**, *41*, 5170–5175. [[CrossRef](#)]
7. Schulz-Harder, J. DBC Substrates as a Base for Power MCM's. *Proc. Electron. Packag. Technol. Conf. EPTC* **2000**, *2000*, 315–320. [[CrossRef](#)]
8. Narumanchi, S.; Mihalic, M.; Kelly, K.; Eesley, G. Thermal Interface Materials for Power Electronics Applications. In Proceedings of the 11th Intersociety Conference on Thermal and Thermomechanical Phenomena in Electronic Systems, Orlando, FL, USA, 28–31 May 2008; pp. 395–404. [[CrossRef](#)]
9. Lin, J.J.; Lin, C.I.; Kao, T.H.; Huang, M.C. Low-Temperature Metallization and Laser Trimming Process for Microwave Dielectric Ceramic Filters. *Materials* **2021**, *14*, 7519. [[CrossRef](#)]
10. Yu, C.; Buttay, C.; Laboure, E. Thermal Management and Electromagnetic Analysis for GaN Devices Packaging on DBC Substrate. *IEEE Trans. Power Electron.* **2017**, *32*, 906–910. [[CrossRef](#)]
11. Yeon, J.; Yamamoto, M.; Ni, P.; Nakamoto, M.; Tanaka, T. Joining of Metal to Ceramic Plate Using Super-Spread Wetting. *Metals* **2020**, *10*, 1377. [[CrossRef](#)]

12. Fukuda, S.; Shimada, K.; Izu, N.; Miyazaki, H.; Iwakiri, S.; Hirao, K. Relationship between the Thermal Stress and Structures of Thermal-Cycling-Induced Cracks in Electroless Nickel Plating on Metalized Substrates. *J. Mater. Sci. Mater. Electron.* **2019**, *30*, 5820–5832. [[CrossRef](#)]
13. Alkaraki, S.; Andy, A.S.; Gao, Y.; Tong, K.F.; Ying, Z.; Donnan, R.; Parini, C. Compact and Low-Cost 3-D Printed Antennas Metalized Using Spray-Coating Technology for 5G Mm-Wave Communication Systems. *IEEE Antennas Wirel. Propag. Lett.* **2018**, *17*, 2051–2055. [[CrossRef](#)]
14. Fontana, A.; Perigaud, A.; Delhote, N.; Carsenat, D.; Acikalin, G.; Richard, P.; Bila, S. Collective Fabrication of LMST Thermally-Stable Surface-Mount Ceramic Devices for Millimeter-Wave Bands. In Proceedings of the 2021 51st European Microwave Conference (EuMC), London, UK, 4–6 April 2021; pp. 688–691. [[CrossRef](#)]
15. Seto, N.; Hirose, S.; Tsuda, H.; Akedo, J. Formation of Tough Foundation Layer for Electrical Plating on Insulator Using Aerosol Deposition Method of Cu-Al₂O₃ Mixed Powder. *Adv. Multifunct. Mater. Syst. II* **2014**, *245*, 17–22. [[CrossRef](#)]
16. Thakare, J.G.; Pandey, C.; Mahapatra, M.M.; Mulik, R.S. Thermal Barrier Coatings—A State of the Art Review. *Met. Mater. Int.* **2021**, *27*, 1947–1968. [[CrossRef](#)]
17. Raelison, R.N.; Xie, Y.; Sapanathan, T.; Planche, M.P.; Kromer, R.; Costil, S.; Langlade, C. Cold Gas Dynamic Spray Technology: A Comprehensive Review of Processing Conditions for Various Technological Developments till to Date. *Addit. Manuf.* **2018**, *19*, 134–159. [[CrossRef](#)]
18. Castillo, H.A.; Restrepo-Parra, E.; De La Cruz, W.; Bixbi, B.; Hernandez, A. CuO Thin Films Produced for Improving the Adhesion between Cu and Al₂O₃ Foils in a Direct Bonded Copper (DBC) Process. *J. Adhes.* **2018**, *94*, 615–626. [[CrossRef](#)]
19. Tumarkin, A.V.; Kaziev, A.V.; Kolodko, D.V.; Pisarev, A.A.; Kharkov, M.M.; Khodachenko, G.V. Deposition of Copper Coatings in a Magnetron with Liquid Target. *Phys. At. Nucl.* **2015**, *78*, 1674–1676. [[CrossRef](#)]
20. Kaziev, A.V.; Tumarkin, A.V.; Leonova, K.A.; Kolodko, D.V.; Kharkov, M.M.; Ageychenkov, D.G. Discharge Parameters and Plasma Characterization in a Dc Magnetron with Liquid Cu Target. *Vacuum* **2018**, *156*, 48–54. [[CrossRef](#)]
21. Bleykher, G.A.; Yuryeva, A.V.; Shabunin, A.S.; Sidelev, D.V.; Grudin, V.A.; Yuryev, Y.N. The Properties of Cu Films Deposited by High Rate Magnetron Sputtering from a Liquid Target. *Vacuum* **2019**, *169*, 8914. [[CrossRef](#)]
22. Andersson, J.; Anders, A. Gasless Sputtering: Opportunities for Ultraclean Metallization, Coatings in Space, and Propulsion. *Appl. Phys. Lett.* **2008**, *92*, 221503. [[CrossRef](#)]
23. Akimoto, K.; Ishizuka, S.; Yanagita, M.; Nawa, Y.; Paul, G.K.; Sakurai, T. Thin Film Deposition of Cu₂O and Application for Solar Cells. *Sol. Energy* **2006**, *80*, 715–722. [[CrossRef](#)]
24. Dolai, S.; Dey, R.; Das, S.; Hussain, S.; Bhar, R.; Pal, A.K. Cupric Oxide (CuO) Thin Films Prepared by Reactive d.c. Magnetron Sputtering Technique for Photovoltaic Application. *J. Alloys Compd.* **2017**, *724*, 456–464. [[CrossRef](#)]
25. Sidelev, D.V.; Voronina, E.D.; Grudin, V.A. High-Rate Magnetron Deposition of CuO_x Films in the Metallic Mode Enhanced by Radiofrequency Inductively Coupled Plasma Source. *Vacuum* **2023**, *207*, 1551. [[CrossRef](#)]
26. Tumarkin, A.V.; Kaziev, A.V.; Kharkov, M.M.; Kolodko, D.V.; Ilychev, I.V.; Khodachenko, G.V. High-Current Impulse Magnetron Discharge with Liquid Target. *Surf. Coatings Technol.* **2016**, *293*, 42–47. [[CrossRef](#)]

Disclaimer/Publisher's Note: The statements, opinions and data contained in all publications are solely those of the individual author(s) and contributor(s) and not of MDPI and/or the editor(s). MDPI and/or the editor(s) disclaim responsibility for any injury to people or property resulting from any ideas, methods, instructions or products referred to in the content.